

# Spindle cell sarcoma with *KIAA1549-BRAF* resembling infantile fibrosarcoma morphologically: A case report and literature review

TOMOKO FUJIKAWA<sup>1</sup>, SUGURU UEMURA<sup>1</sup>, MAKIKO YOSHIDA<sup>2</sup>, SAYAKA HYODO<sup>1</sup>, AIKO KOZAKI<sup>1</sup>, ATSURO SAITO<sup>1</sup>, KENJI KISHIMOTO<sup>1</sup>, TOSHIKI ISHIDA<sup>1</sup>, TAKESHI MORI<sup>1</sup>, AYANO UEMATSU<sup>3</sup>, KEIICHI MORITA<sup>3</sup>, TADASHI HATAKEYAMA<sup>3</sup>, AKIHIRO TAMURA<sup>4</sup>, NOBUYUKI YAMAMOTO<sup>4</sup>, MASATO KOMATSU<sup>5</sup>, TOSHINORI SOEJIMA<sup>6</sup>, DAIICHIRO HASEGAWA<sup>1</sup> and YOSHIYUKI KOSAKA<sup>1</sup>

Departments of <sup>1</sup>Hematology and Oncology, <sup>2</sup>Pathology, and <sup>3</sup>Surgery, Kobe Children's Hospital, Kobe, Hyogo 650-0047;

Departments of <sup>4</sup>Pediatrics and <sup>5</sup>Pathology, Kobe University Graduate School of Medicine, Kobe, Hyogo 650-0017;

<sup>6</sup>Department of Radiation Oncology, Kobe Proton Center, Kobe, Hyogo 650-0047, Japan

Received September 7, 2022; Accepted October 18, 2022

DOI: 10.3892/ol.2022.13572

**Abstract.** Infantile fibrosarcoma (IFS) commonly harbors ETS variant transcription factor 6 (*ETV6*)-neurotrophic receptor tyrosine kinase 3 (*NTRK3*) fusion. However, the recent accessibility to clinical next-generation sequencing (NGS) has revealed *ETV6-NTRK3* negative spindle cell sarcomas resembling IFS morphologically, involving *NTRK1/2*, *MET*, *RET* and *BRAF*. The present report describes a pediatric case of spindle cell sarcoma with *KIAA1549-BRAF* resembling IFS morphologically. A 20-month-old female patient was referred to Kobe Children's Hospital (Kobe, Japan) for the treatment of intrathoracic spindle cell sarcoma. Pathologically, the intrathoracic tumor cells were composed of spindle cells with focal hemangiopericytomatous pattern. In immunohistochemistry analysis, the intrathoracic tumor cells focally expressed desmin and WT-1 and were negative for pan-tropomyosin receptor kinase (TRK), S-100 and CD34. Fluorescence *in situ* hybridization analysis for *ETV6* and capicua transcriptional repressor revealed negative split signals. Although the patient was initially diagnosed with IFS morphologically, *KIAA1549-BRAF* fusion transcript was detected by comprehensive genomic profiling with NGS using intrathoracic tumor tissues and confirmed by reverse transcription-PCR. Chemotherapy induced a reduction in the tumor size. At present, the patient is alive with the disease and has been receiving therapy for 8 months since the initiation of chemotherapy. Review of *BRAF*-altered spindle cell sarcomas resembling IFS

morphologically revealed the inconsistency in immunohistochemical expression patterns and the diversity of *BRAF* fusion genes and mutations. Therefore, the elucidation of genomic profiling by NGS may assist in making an appropriate diagnosis and selecting novel alternative therapies in *ETV6-NTRK3*-negative spindle cell sarcomas resembling IFS morphologically.

## Introduction

Infantile fibrosarcoma (IFS) is a malignant fibroblastic tumor and occurs in younger children under the age of 2 years (1,2). IFS occurs most frequently in the extremities or trunk and less frequently in the abdomen or the retroperitoneum. Metastasis at diagnosis is uncommon (<4%) (1,2). IFS is pathologically described as hypercellular tumors comprising monomorphic spindle cells with scant cytoplasm, including a hemangiopericytoma-like vascular pattern (3). The immunohistochemistry demonstrates the variable expression patterns of smooth muscle actin (SMA), CD34, S100, and CD30 (4,5). Most cases of IFS harbor an *ETV6-NTRK3* gene fusion, resulting in the expression of pan-TRK in the immunohistochemistry (2,6).

The recent accessibility to clinical next-generation sequencing (NGS) revealed *ETV6-NTRK3* negative spindle cell sarcomas resembling IFS morphologically. The spindle cell sarcomas described above involve other kinase genes such as *NTRK1/2*, *RET*, *MET*, and *BRAF*, each with various gene partners (7-11).

*BRAF* encodes a serine/threonine RAF kinase, regulates the MAP kinase/ERK signaling pathway, and causes tumorigenesis. In some solid tumors and hematological malignancies, the activating mutations in *BRAF*, typically resulting in V600E were identified and emerged as potential therapy targets (12,13). However, the biological and clinical characteristics of *BRAF*-altered spindle cell sarcomas resembling IFS morphologically remain to be elucidated. Herein, we report a pediatric case of spindle cell sarcoma with *KIAA1549-BRAF* resembling IFS morphologically.

---

**Correspondence to:** Dr Suguru Uemura, Department of Hematology and Oncology, Kobe Children's Hospital, Minatojima-minanimachi 1-6-7, Chuo-ku, Kobe, Hyogo 650-0047, Japan  
E-mail: sguemura\_kch@hp.pref.hyogo.jp

**Key words:** infantile fibrosarcoma, *KIAA1549-BRAF*, spindle cell sarcoma, sarcoma, next-generation sequencing

## Case report

A 20-month-female was transferred to our hospital for the treatment of an intrathoracic tumor. She had no remarkable family history. At the age of 3 weeks, a subcutaneous tumor in the right buttock was incidentally noted by a family doctor. Because the tumor gradually increased in size, the total resection of the tumor was performed at the age of 12 months. She was diagnosed with IFS and followed up care without any additional therapies. However, she relapsed as left intrathoracic tumors at the age of 20 months. The enhanced computed tomography (CT) at transfer showed left intrathoracic tumor of 5x4 cm with severe mediastinal shift, as well as right intrathoracic tumor of 1.5x1.5 cm (Fig. 1A and B). Enhanced CT with 5 mm slice thickness was performed using 640-multislice CT scanners (Aquilion ONE, Canon Medical Systems Corporation, Otawara, Japan). Iopamiron® (Bayer, Osaka, Japan) was used as iodinated contrast medium. No other metastatic diseases were detected. The biopsy of the left intrathoracic tumor revealed the presence of IFS. The VDC-IE chemotherapy containing vincristine, doxorubicin, cyclophosphamide, ifosfamide, and etoposide, induced a significant reduction in tumor size. She was alive with disease receiving therapy for 8 months since the initiation of chemotherapy.

The tumor cells were composed of spindle cells, arranged into intersecting fascicles with focal hemangiopericytomatous pattern (Fig. 2A). The mitoses in the tumor were counted at 10 per 10 high-power fields (Fig. 2B). The procedure of H&E pathological staining was as follows. Resected specimens were immediately fixed with 10% formalin neutral buffer solution for 48 h at room temperature. Fixed sections were embedded in paraffin and 4- $\mu$ m-thick tissue sections were stained with hematoxylin and eosin solutions (Sakura, Tokyo, Japan). Immunohistochemical staining was performed on 4- $\mu$ m-thick sections using a fully automated systems [Bench Mark GX System (Roche, Rotkreuz, Switzerland) or Leica Bond-max (Leica Biosystems, Buffalo Grove, IL, USA)] and the following primary antibodies; desmin (clone D33; prediluted) (IR606; Dako, Carpinteria, CA, USA), Wilms tumor gene 1 (WT-1) (6F-H2; dilution 1:1) (41386; NICHIREI, Osaka, Japan), pan-TRK [VENTANA Pan-TRK (EPR17341) Assay] (790-7026; Roche), S-100 (polyclonal; dilution 1:2,000) (Z3011; Dako), SMA (clone 1A4; dilution 1:300) (IR611; Dako), CD34 (clone NU-4A1; dilution 1:4) (41311; NICHIREI, Osaka Japan), CD99 (clone O13; prediluted) (790-4452; Roche), NK2 homeobox 2 (NKX2.2) (rabbit polyclonal; dilution 1:50) (NBPI-82554; Novus Biologicals, Littleton, CO, USA), myogenic differentiation 1 (MyoD1) (mouse monoclonal; dilution 1:250) (ab133627, abcam, USA), and pan-cytokeratin (clone AE1/AE3; dilution 1:100) (IR053; Dako). The reaction of secondary antibody and following DAB (3,3'-Diaminobenzidine) reaction were performed using ultraView Universal DAB detection kit (109431; Roche) for Bench Mark GX System or BOND Polymer Refine Detection (DS9800; Leica Biosystems) for Leica Bond-max. Appropriate positive control sections were mounted on the same slide glasses. By immunohistochemistry, the right buttock and left intrathoracic tumor cells focally expressed desmin (Fig. 3A). WT-1 was detected in the cytoplasm of tumor cells, not nucleus (Fig. 3B). The both tumor cells were negative for pan-TRK, S-100, SMA, CD34, CD99,

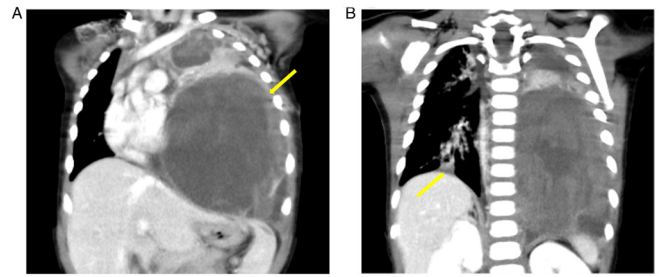


Figure 1. Images of enhanced computer tomography. (A) Left intrathoracic tumors (arrow) with severe mediastinal shift. (B) Right intrathoracic tumor (arrow).

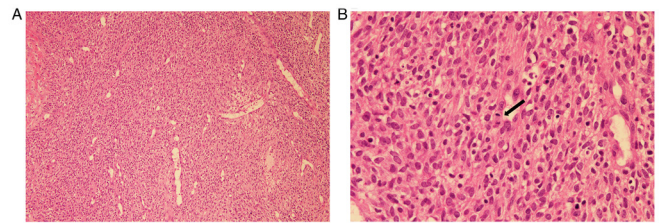


Figure 2. Histopathological images of intrathoracic tumor stained with hematoxylin and eosin. (A) The tumor was composed of spindle cells with hemangiopericytomatous patterns (magnification, x100). (B) Tumor cells were monomorphic and ovoid to spindle with mitoses (arrow) (magnification, x400).

NKX2.2, MyoD1, and pan-cytokeratin (Fig. 3C-J). Interphase fluorescence *in situ* hybridization (FISH) was extracted from formalin-fixed paraffin-embedded tissue (FFPE). ETV6 break apart probe (Vysis LSI ETV6 Dual Color, Break Apart Probe Kit) (VYSIS/Abbott, Abbott Park, IL) was used for the detection of rearrangement of ETV6 (12p13). The Sure FISH CIC 5' BA probe and the Sure FISH CIC 3' BA probe (Agilent Technologies, Cedar Creek, USA) were used for the detection of CIC (19q13.2) rearrangement. FISH analysis for *ETV6* and *CIC* revealed negative split signals in the right buttock tumor cells. Using the left intrathoracic tumor tissues, *KIAA1549-BRAF* fusion transcript was identified by the comprehensive genomic profiling with NGS-FoundationOne™, which examines the whole coding sequence of 315 cancer-related genes and introns from 28 genes often rearranged or altered in cancer. Other genomic alterations identified using FoundationOne™ were *STK11* F354L and *RET* A45V. Subsequently, *KIAA1549-BRAF* fusion transcript was confirmed by reverse transcription-polymerase chain reaction (RT-PCR) (Fig. 4A). While several types of *KIAA1549-BRAF* fusion transcripts were previously reported (14), the transcript composed of *KIAA1549* exon 10 fused to *BRAF* exon 9 was exclusively detected in our case (Fig. 4B). The procedure of sanger sequence was as follows. RNA was extracted from FFPE tissue of the right buttock tumor using The RNastorm™ kit (Cell Data Science, CA, USA). For RT-PCR, cDNA was synthesized from 1.0  $\mu$ g of total RNA using a SuperScript™ IV First-Strand Synthesis System (ThermoFisher Scientific, Oslo, Norway). PCR reaction was performed using a GoTaq® DNA polymerase (Promega, WI, USA) with *KIAA1549*-forward (5'-GATTGTTGTCATCCTCTACTGG-3') and *BRAF*-reverse (5'-CCTCCATCACCACGAAATCCTT-3') primers. PCR conditions were initial denaturation at 95°C for 1 min, 40 cycles

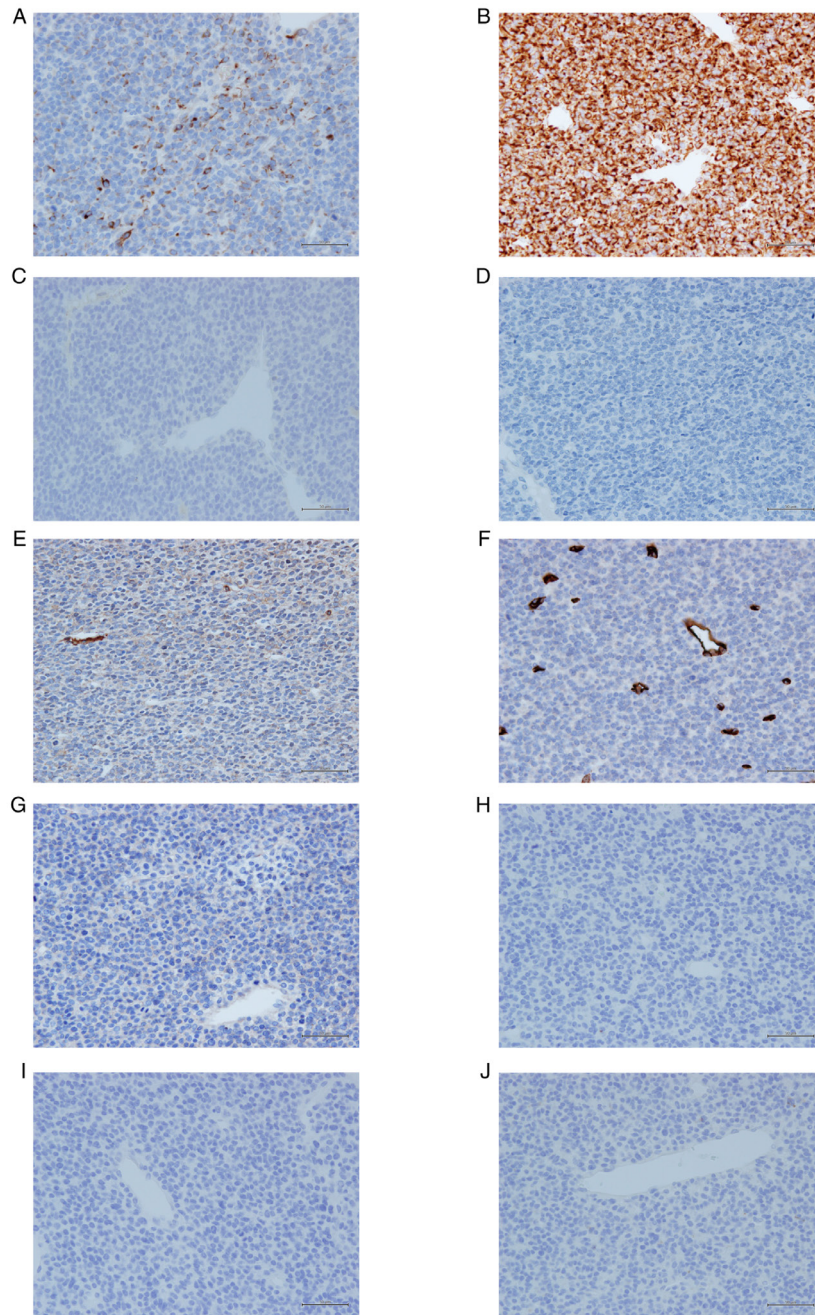


Figure 3. IHC staining (magnification, x400). (A) Weak positive expression of desmin. (B) Cytoplasmic expression of WT-1. Negative IHC staining results for (C) pan-TRK, (D) S-100, (E) SMA, (F) CD34, (G) CD99, (H) NKX2.2, (I) MyoD1 and (J) pan-cytokeratin. IHC, immunohistochemistry; WT-1, wilms tumor gene 1; pan-TRK, pan-tropomyosin receptor kinase; SMA, smooth muscle actin; NKX2.2, NK2 homeobox 2; MyoD1, myogenic differentiation 1.

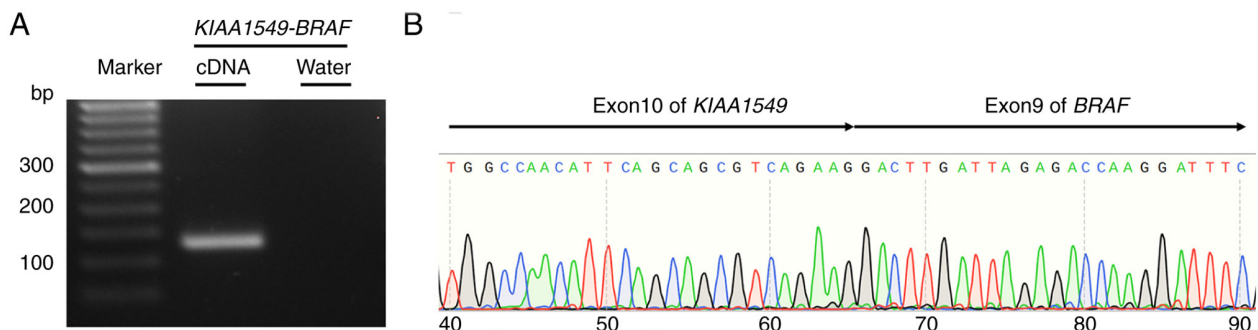


Figure 4. *KIAA1549-BRAF* fusion protein. (A) RT-PCR of *KIAA1549-BRAF* fusion transcript. RT-PCR was performed with *KIAA1549*-forward (5'-GATTGTTGTCATCCTCTACTGG-3') and *BRAF*-reverse (5'-CCTCCATCACCACGAAATCCTT-3') primers. (B) RT-PCR followed by sequencing analysis revealed that exon 10 of *KIAA1549* was fused to the sequence within exon 9 of *BRAF*. RT-PCR, reverse transcription-PCR.

of 95°C for 30 sec, annealing at 51°C for 30 sec, 72°C for 30 sec, and a final extension at 72°C for 5 min. PCR products were electrophoresed on 2.0% agarose gel and purified with Wizard® SV Gel and PCR Clean-up System (Promega, WI, USA). BigDye Terminator v3.1 Cycle Sequencing kit (Thermo Scientific, USA) was used for terminator cycling sequencing reactions for Sanger sequencing of purified PCR products on the 3730xl DNA Analyzer (Thermo Fisher Scientific, USA).

## Discussion

Herein, we reported a pediatric case of spindle cell sarcoma with *KIAA1549-BRAF* resembling IFS morphologically. Although the present case was initially diagnosed with IFS morphologically, a comprehensive genomic profiling with NGS led to a more precise diagnosis. Because sarcomas in pediatrics are rare and heterogenous, the elucidation of genomic profiling in pediatric sarcomas using NGS can contribute to an appropriate diagnosis and targetable therapies.

The characteristics of *BRAF*-altered spindle cell sarcomas resembling IFS morphologically are not well understood (10,11,15-18). To identify the clinical characteristics of *BRAF*-altered spindle cell sarcomas resembling IFS morphologically, we conducted a literature search of all reports. A literature search of all reports was conducted. The following keywords were used in the electronic databases PubMed with no date of publication limitations: 'infantile fibrosarcoma' OR 'spindle cell sarcoma' OR 'spindle cell neoplasm' combined with 'BRAF'. From the titles and abstracts, we excluded non-English language studies, meeting presentations, and commentaries. The article titles, abstracts, and full papers were examined, and the reports not containing *BRAF*-altered IFS, spindle cell sarcoma, or spindle cell neoplasm were excluded. URL was as follows: [https://pubmed.ncbi.nlm.nih.gov/?term=\(\(infantile%20fibrosarcoma\)%20OR%20\(spindle%20cell%20sarcoma\)%20OR%20\(spindle%20cell%20neoplasm\)\)\)%20AND%20\(BRAF\)&sort=date](https://pubmed.ncbi.nlm.nih.gov/?term=((infantile%20fibrosarcoma)%20OR%20(spindle%20cell%20sarcoma)%20OR%20(spindle%20cell%20neoplasm)))%20AND%20(BRAF)&sort=date)

We identified 24 cases of spindle cell sarcoma with *BRAF*-rearrangement or mutation. The median age at diagnosis was 5.5 months (range: 0-69 years). Seven of 24 cases (30%) were diagnosed over 2 years of age and in three cases over 20 years of age. The most common site of tumors was extremities (6 cases, 25%). Immunohistochemical identification of expression of CD34 was observed in 8 (47%) cases, S-100 in 4 (21%) cases, and SMA in 6 (40%) cases. The expression of pan-Trk was present in one (9.0%) case. *BRAF*-rearrangements, including fusions of *BRAF* kinase domain, were detected in 17 cases (68%). The fusions were as follows: *KIAA1549-BRAF*, *AGAP3-BRAF*, *CUX1-BRAF*, *DAAMI-BRAF*, *EPB4IL2-BRAF*, *MCC-BRAF*, *NPFI-BRAF*, *OSBP-BRAF*, *PDE10A-BRAF*, *SEPT7-BRAF*, *TEX4-BRAF*, *FOXN3-BRAF*, and *TRIP11-BRAF* (10,11,15-18). *KIAA1549-BRAF* fusion was detected in two cases as in our case (10,19). *BRAF* point mutations were present in four cases and *BRAF*-internal duplication (ID) in three cases (10,16,17). One case contained *BRAF* point mutation and *BRAF*-rearrangement. The identification of *ETV6-NTRK3* transcript was performed in 12 cases by FISH for *ETV6* or whole genome sequencing. In two cases, *ETV6-NTRK3* fusion and *BRAF*-ID coexisted (17). One case

harbored two distinct *BRAF* fusions (*FOXN3-BRAF* and *TRIP11-BRAF*) (10). Three of 13 cases (23%) had metastasis at diagnosis. All the three cases occurred in adults and were refractory to the conventional chemotherapy. Median follow-up period was 10 months (3-60 months) and 2 patients (8%) died of disease. In our review of *BRAF*-altered spindle cell sarcomas resembling IFS morphologically, most cases occurred in younger children under the age of 2 years, showed nonspecific patterns of immunohistochemistry staining, and harbored a *BRAF* fusion. These results were consistent with our case.

*KIAA1549-BRAF* fusion is considered as a recurrent oncogenic driver in pilocytic astrocytoma (19). *KIAA1549-BRAF* fusion leads to loss of N-terminal regulatory domain of *BRAF* and subsequent activation of the kinase domain, thereby resulting in constitutive activation of *BRAF* (20). Although different fusion variants were identified in *KIAA1549-BRAF*, the transcript detected in our case was composed of *KIAA1549* exon 10 fused to *BRAF* exon 9 and contained the intact *BRAF* kinase domain. Trametinib, a MEK inhibitor has recently been demonstrated to be effective in low-grade glioma with *BRAF* fusions including *KIAA1549-BRAF* (21,22). Subbiah *et al* (15) reported the effectiveness of the combination therapy of sorafenib, temsirolimus, and bevacizumab for a spindle cell sarcoma with *KIAA1549-BRAF*, which was refractory to the conventional chemotherapies. Because of limited data, further studies are needed to determine the effectiveness of *BRAF*-targeted therapy including MEK inhibitor for *BRAF*-altered spindle cell sarcomas morphologically resembling IFS.

In conclusion, we report a pediatric case of spindle cell sarcoma with *KIAA1549-BRAF* morphologically resembling IFS. The elucidation of genomic profiling by NGS may assist us in making an appropriate diagnosis and selecting new therapeutic options for *ETV6-NTRK3* negative spindle cell sarcomas morphologically resembling IFS.

## Acknowledgements

Not applicable.

## Funding

No funding was received.

## Availability of data and materials

The dataset used and/or analyzed during the current study are available from the corresponding author on reasonable request.

## Authors' contributions

TF, SU, MY, DH and YK participated in the conception and design of the study. MY, SH, AK, AS, KK, TI, AU, KM, TH, MK, and TS were involved in the analysis and interpretation of the data for the pathological diagnosis. MY, TM, AT, NY, MK and TS were involved in the analysis and interpretation of data for comprehensive genomic profiling using NGS. AU, KM and TH performed surgery. MY and MK performed the

histological examination of the tumors. TF and SU drafted the initial manuscript. TF, SU, MY, KK, MK, DH and YK critically revised the article for important intellectual content. TH, TS, DH and YK confirmed the authenticity of all the raw data. All authors have read and approved the final manuscript.

### Ethics approval and consent to participate

The present study was approved by the Institutional Review Board of Kobe Children's Hospital (R3-62; Kobe, Japan). Written informed consent was obtained from the patient's parents.

### Patient consent for publication

The patient's parents provided written informed consent for the publication of any associated data.

### Competing interests

The authors declare that they have no competing interests.

### References

- Orbach D, Rey A, Cecchetto G, Oberlin O, Casanova M, Thebaud E, Scopinaro M, Bisogno G, Carli M and Ferrari A: Infantile fibrosarcoma: Management based on the European experience. *J Clin Oncol* 28: 318-323, 2010.
- Orbach D, Brennan B, De Paoli A, Gallego S, Mudry P, Francotte N, van Noesel M, Kelsey A, Alaggio R, Ranchère D, *et al*: Conservative strategy in infantile fibrosarcoma is possible: The European paediatric soft tissue sarcoma study group experience. *Eur J Cancer* 57: 1-9, 2016.
- Chung EB and Enzinger FM: Infantile fibrosarcoma. *Cancer* 38: 729-739, 1976.
- Davis JL, Lockwood CM, Stohr B, Boecking C, Al-Ibraheemi A, DuBois SG, Vargas SO, Black JO, Cox MC, Luquette M, *et al*: Expanding the spectrum of pediatric NTRK-rearranged mesenchymal tumors. *Am J Surg Pathol* 43: 435-445, 2019.
- Coffin CM, Jaszcz W, O'Shea PA and Dehner LP: So-called congenital-infantile fibrosarcoma: Does it exist and what is it? *Pediatr Pathol* 14: 133-150, 1994.
- Rudzinski ER, Lockwood CM, Stohr BA, Vargas SO, Sheridan R, Black JO, Rajaram V, Laetsch TW and Davis JL: Pan-Trk immunohistochemistry identifies NTRK rearrangements in pediatric mesenchymal tumors. *Am J Surg Pathol* 42: 927-935, 2018.
- Pavlick D, Schrock AB, Malicki D, Stephens PJ, Kuo DJ, Ahn H, Turpin B, Allen JM, Rosenzweig M, Badizadegan K, *et al*: Identification of NTRK fusions in pediatric mesenchymal tumors. *Pediatr Blood Cancer* 64: e26433, 2017.
- Davis JL, Vargas SO, Rudzinski ER, López Marti JM, Janeway K, Forrest S, Winsnes K, Pinto N, Yang SE, VanSandt M, *et al*: Recurrent RET gene fusions in paediatric spindle mesenchymal neoplasms. *Histopathology* 76: 1032-1041, 2020.
- Flucke U, van Noesel MM, Wijnen M, Zhang L, Chen CL, Sung YS and Antonescu CR: TFG-MET fusion in an infantile spindle cell sarcoma with neural features. *Genes Chromosomes Cancer* 56: 663-667, 2017.
- Penning AJ, Al-Ibraheemi A, Michal M, Larsen BT, Cho SJ, Lockwood CM, Paulson VA, Liu YJ, Plank L, Fritchie K, *et al*: Novel BRAF gene fusions and activating point mutations in spindle cell sarcomas with histologic overlap with infantile fibrosarcoma. *Mod Pathol* 34: 1530-1540, 2021.
- Kao YC, Fletcher CDM, Alaggio R, Wexler L, Zhang L, Sung YS, Orhan D, Chang WC, Swanson D, Dickson BC and Antonescu CR: Recurrent BRAF gene fusions in a subset of pediatric spindle cell sarcomas: Expanding the genetic spectrum of tumors with overlapping features with infantile fibrosarcoma. *Am J Surg Pathol* 42: 28-38, 2018.
- El-Osta H, Falchook G, Tsimberidou A, Hong D, Naing A, Kim K, Wen S, Janku F and Kurzrock R: BRAF mutations in advanced cancers: Clinical characteristics and outcomes. *PLoS One* 6: e25806, 2011.
- Davies H, Bignell GR, Cox C, Stephens P, Edkins S, Clegg S, Teague J, Woffendin H, Garnett MJ, Bottomley W, *et al*: Mutations of the BRAF gene in human cancer. *Nature* 417: 949-954, 2002.
- Ross JS, Wang K, Chmielecki J, Gay L, Johnson A, Chudnovsky J, Yelensky R, Lipson D, Ali SM, Elvin JA, *et al*: The distribution of BRAF gene fusions in solid tumors and response to targeted therapy. *Int J Cancer* 138: 881-890, 2016.
- Subbiah V, Westin SN, Wang K, Araujo D, Wang WL, Miller VA, Ross JS, Stephens PJ, Palmer GA and Ali SM: Targeted therapy by combined inhibition of the RAF and mTOR kinases in malignant spindle cell neoplasm harboring the KIAA1549-BRAF fusion protein. *J Hematol Oncol* 7: 8, 2014.
- Mitsis D, Opyrchal M, Zhao Y, Kane Iii JM, Cheney R and Salerno KE: Exceptional clinical response to BRAF-targeted therapy in a patient with metastatic sarcoma. *Cureus* 7: e439, 2015.
- Wegert J, Vokuhl C, Collord G, Del Castillo Velasco-Herrera M, Farndon SJ, Guzzo C, Jorgensen M, Anderson J, Slater O, Duncan C, *et al*: Recurrent intragenic rearrangements of EGFR and BRAF in soft tissue tumors of infants. *Nat Commun* 9: 2378, 2018.
- Hughes CE, Correa H, Benedetti DJ, Smith B, Sumegi J and Bridge J: Second report of PDE10A-BRAF fusion in pediatric spindle cell sarcoma with infantile fibrosarcoma-like morphology suggesting PDE10A-BRAF fusion is a recurrent event. *Pediatr Dev Pathol* 24: 554-558, 2021.
- Zhang J, Wu G, Miller CP, Tatevossian RG, Dalton JD, Tang B, Orisme W, Punchihewa C, Parker M, Qaddoumi I, *et al*: Whole-genome sequencing identifies genetic alterations in pediatric low-grade gliomas. *Nat Genet* 45: 602-612, 2013.
- Jones DT, Kocialkowski S, Liu L, Pearson DM, Bäcklund LM, Ichimura K and Collins VP: Tandem duplication producing a novel oncogenic BRAF fusion gene defines the majority of pilocytic astrocytomas. *Cancer Res* 68: 8673-8677, 2008.
- Selt F, van Tilburg CM, Bison B, Sievers P, Harting I, Ecker J, Pajtlér KW, Sahm F, Bahr A, Simon M, *et al*: Response to trametinib treatment in progressive pediatric low-grade glioma patients. *J Neurooncol* 149: 499-510, 2020.
- Perreault S, Larouche V, Tabori U, Hawkin C, Lippé S, Ellezam B, Décarie JC, Théoret Y, Métras ME, Sultan S, *et al*: A phase 2 study of trametinib for patients with pediatric glioma or plexiform neurofibroma with refractory tumor and activation of the MAPK/ERK pathway: TRAM-01. *BMC Cancer* 19: 1250, 2019.



This work is licensed under a Creative Commons Attribution-NonCommercial-NoDerivatives 4.0 International (CC BY-NC-ND 4.0) License.